canopy air heat balance, convection heat delivery with leaf side as well as advection of outside air and inside plant canopy are considered. On the other hand, as for moist transfer, absorption moist from soil, moist transfer to upper roots and stems, moist transfer from leaves to canopy air are considered for plant roots. Concerning canopy air, moist transfer from leaves, outside air and advection inside canopy are considered. But in the uppermost layer plant canopy, outside air is transferred to leaf top, while canopy air and heat・moist are transferred to lower leaf. Also, outside air and heat・moist are considered according to the intra-plant canopy-layer advection.

Long-Wavelength Radiation Heat Receiving in Plant Layer

Regarding the effective radiation penetration of each virtually hypofractionated plant canopy, long-wave radiation and attenuation coefficient changing according to the plant leaf direction are considered. Considering the long-wavelength radiation heat received by canopy layer plant. Plant canopy formed from upper/lower layer and mutual radiation with air are considered.

A Solar Radiation Heat Absorption in Plant Layer

The appearance of solar radiation absorption, reflexibility, penetration of each plant canopy was calculated based on the solar radiation multiple reflections/absorption results between plant canopies. The heat amount of solar radiation in each layer was calculated by one outlying value of plant canopy layer multiplied by the solar radiation absorption considering incidence solar radiation and multiple reflections/absorption.

Heat and Water transfer in Plant Layer

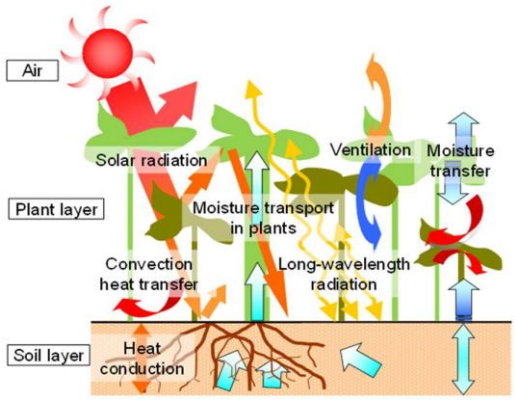

Figure 3. Heat and Water Transfer

The intra-canopy air current speed was expressed as exponential law and continuous system, motion equation, and energy equation by using the air current speed of outside air. Leaf and surface heat・moist transfer ratio were calculated by using boundary layer theory and heat transfer and matter transfer analogue though the dimensionless equation. As for convection heat transfer rate, the Nu values of forced convection and natural convection were compared and a larger one was used. Concerning the wind speed during Re value calculation, outdoor wind speed 0.3m above canopy was used. As for the intra-canopy, the mean flow velocity of each virtually hypofractionated canopy was utilized. The amount of plant-canopy moist transfer was expressed as the sum of leaf moist transfer amount and soil moist transfer emission amount. If the moist potential difference is expressed as driving force, plant-leaf appearance moist transfer rate and soil moist transfer rate can be used to calculate the moist transfer amount. But, the leaf moist transfer rate is affected by the moist transfer rate of leaf boundary layer and the moist transfer rate of stoma. The stoma moist transfer rate relies on stoma openness. On the other hand, the moist transfer rate of leaf boundary layer relies on wind speed.

The Effect of the Temperature Rise

Table 2. Calculation condition for Temperature rise

	Term of caluculation	Temperture rise
Before urbanization	1940～1960 (For 20years)	×
After Urbanization	1960～2010 (For 50years)	○

First of all, underground temperature before urbanization was reproduced, which is deemed to be a cause of underground warming.

Calculation conditions are described in Table 2. Until 50 years ago, urbanization was not existent. Therefore no temperature increase was assumed and surface cover composition was supposed green. In the case, the results of underground temperature calculation are shown in Figure 4. At around 10m-deep point, underground temperature was 16˚C, showing an almost constant level.

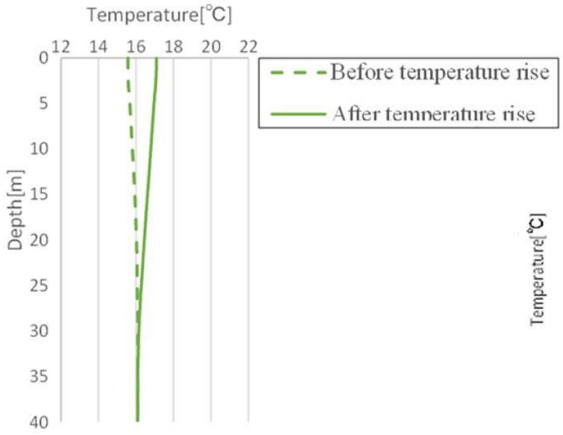

Figure 4. Results of underground temperature calculation

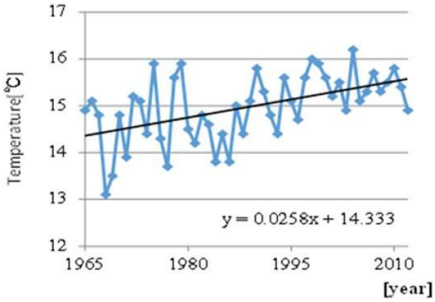

Figure 5. Annual average air temperature in Hadano City

In this condition temperature increase was assumed to have taken place from 50 years before in performing the calculation until now (for 50 years). As for temperature increase, based on the yearly average temperature data since 1965 observed by Hadano City fire department in Figure 5., a model with the expanded AMEDAS metrological data plus temperature increase adjustment was used. The results of underground temperature calculation affected by temperature increase are displayed in Figure 4. Due to temperature increase, yearly average surface temperature rose by 1.5˚C. This is a trend similar to the 50-year-long temperature increase rate. Also, it is found that up to 28m depth, temperature increased to cause inclination in underground temperature.

The Effect of Ground Cover Changing

Temperature increase effects were not enough to reproduce the warming and temperature inclination, etc. at a deep-seated layer shown in underground temperature distribution. In this sense, this research reviewed the effects of changes in surface cover. In this review, the surface cover composition 50 years ago was assumed to change from green to non-green for calculation. In greens, heat・moist transfer is calculated by setting the surface layer as an unsaturated moist zone calculation in order to consider surface-layer transpiration effects. Nongreens were divided into two types. In barren spaces, permeable layer is set and in asphalt, non-permeable layer is

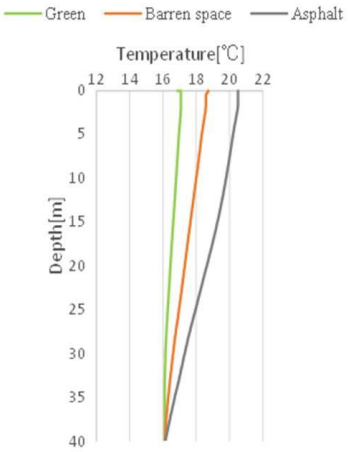

Figure 6. Surface composition -specific underground temperature

set without moist transfer. Also, in all surface layers, deep-seated layers are set as a saturated moist zone. Figure 6. shows surface composition-specific underground temperatures. If green changes into barren space, surface temperature rose by 2.1˚C and the temperature inclination in deep-seated layer grew larger. As shown in Figure 7. on yearly added latent heat amounts, it seems because plant transpiration amount controlled green surface temperature increase. Also Figure 8. shows that the yearly added solar radiation absorption according to each surface cover composition has almost no difference between green and barren space. But asphalt and barren space exhibited about 22% difference.

This difference makes asphalt surface temperature rise by about 1.8˚C compared with barren space while affecting the deep-seated layer warming.

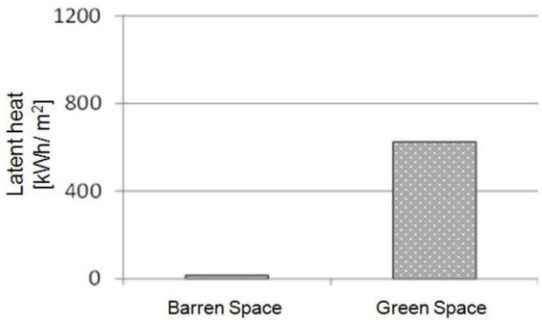

Figure 7. Amount of added latent heat for a year

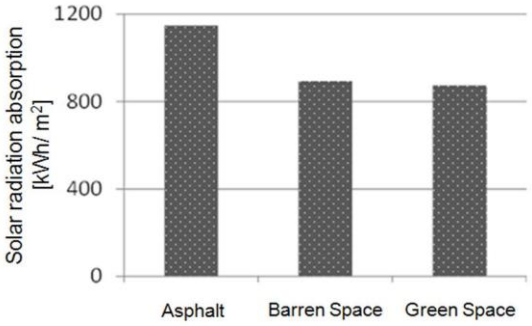

Figure 8. Amount of total solar radiation absorption for a year

Moreover, in order to reproduce the present underground temperature distribution, the characteristics of nearby areas of the targeted calculation place need to be reflected. Green and non-green spaces are mixed in such nearby areas. Thus, the 100m-radius area from the target place was divided every 20m. Based on the underground temperature distribution calculated at each point, 3D heat effects were reflected. Figure 9. shows the land use of the corresponding area based on GIS. The building-caused incidence solar radiation saving in non-green zones reflected in the solar radiation absorption calculated by setting building-part solar radiation absorption at 0.0, and other asphalt paper solar radiation absorption at 0.9 and using the area-weighed average values. Figure 10. exhibits the foresaid calculation method-based yearly average underground temperature distribution as well as actually-measured yearly average underground temperature distribution. The two graphs almost coincide with the precision of numerical simulation.

According to these results, urbanization-led temperature increase and surface cover composition change were found to have warmed up underground to cause underground temperature inversion.

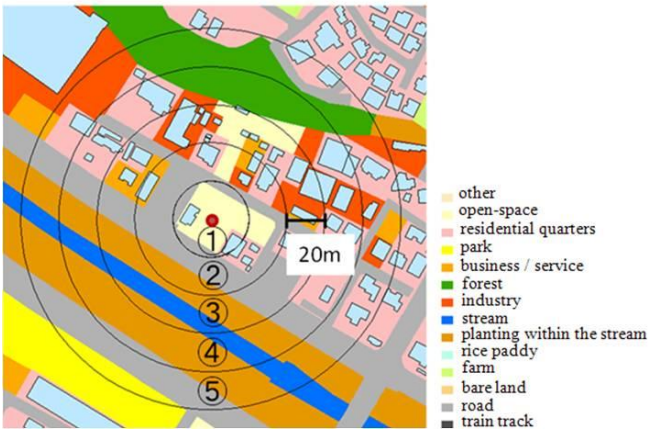

Figure 9. Land use of the corresponding area based on GIS

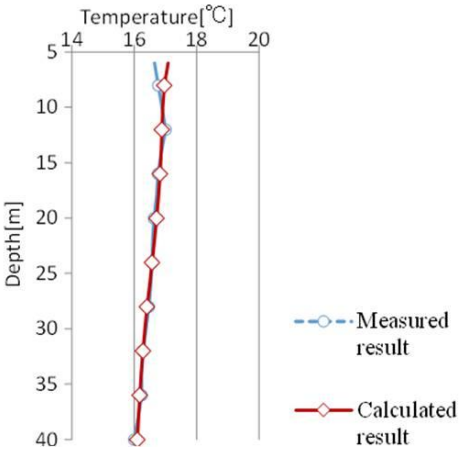

Figure 10. Calculation method-based yearly average underground temperature

CONCLUSIONS

This study, for the purpose of "factor analysis of underground warming", measured underground temperatures of observation wells buried in Hadano City. To clarify causes of underground warming found during the measurement, the heat・moist・air combined transfer model based on air-plant-soil coupling was used to perform the numerical simulation. Hadano City pre-urbanization underground temperature distribution was reproduced with numerical calculation. And based on the status, this study analyzed the effects on underground temperature of urbanization-led surface composition changes and temperature increase deemed as a factor of underground warming. Also by using the GIS, local characteristics of nearby calculation areas such as surface composition were reflected. The underground temperature distribution and underground warming gained in this process were reproduced and compared with actual measurements to check for the accuracy of numerical simulation. By doing so, underground warming was found to have been largely affected by urbanization-led temperature increase and surface composition changes.

【acknowledgment】This research is a part of result of KAKENHI(23246100) "Systematized study on urban planning based on environmental engineering in response to global climate change" (Leader of research: Satoru Sadohara (Yokohama National University)) and the Sumitomo Foundation Research Grant "Development of the Method and Tool that Realizes Water Thermal Energy Circulation Synthesis Management for a Future City of the Global Environment Age" (Leader of research: Satoru Sadohara(Yokohama National University)).

REFERENCES

1) Matsuda C, Ozaki A., et al.: 'Heat and Moisture Transfer and Airflow at Air-Plant-Soil-Continuous System Influence of differences of ground cover specifications on microclimate', Architecture Institute of Japan, 40th The heat symposium, p191-198,2010

2) Ozaki A., Watanabe T., et al.: 'Systematic Analysis on Combined Heat and Water Transfer through Porous Materials Based on Thermodynamic Energy', International Journal of Energy and Buildings, Vol. 33, No.4, 341-350,2001

3) Youhei Uchida and Yasuo Sakura : 'Subsurface temperature profiles in the Nobi Plain', central Japan. *Bull. Geol. Surv. Japan*, vol.50(10), p.635-659, 11 figs., 1 table, 41 appendix-figs.